Ionics (2016) 22:1947–1955
DOI 10.1007/s11581-016-1708-z

ORIGINAL PAPER

Molecularly imprinted polymer based potentiometric sensor for the determination of 1-hexyl-3-methylimidazolium cation in aqueous solution

Kelei Zhuo[1] · Xueli Ma[1] · Yujuan Chen[1] · Congyue Wang[1] · Aoqi Li[1] · Changling Yan[1]

Received: 10 March 2016 / Revised: 2 April 2016 / Accepted: 5 April 2016 / Published online: 18 April 2016

Abstract The molecular imprinting technique is powerful to prepare functional materials with molecular recognition properties. In this work, a potentiometric sensor was fabricated by dispersing molecularly imprinted polymers (MIPs) into plasticized PVC matrix and used for the determination of 1-hexyl-3-methylimidazolium cation ($[C_6mim]^+$) in aqueous solution. The MIPs were synthesized by precipitation polymerization using 1-hexyl-3-methylimidazolium chloride ($[C_6mim]Cl$) as the template molecule, methacrylic acid (MAA) and ethylene glycol dimethacrylat (EGDMA) as the functional monomers, and EGDMA also as the cross-linking agent. The as-prepared electrode exhibited a Nernstian response (58.87 ± 0.3 mV per decade) to $[C_6mim]^+$ in a concentration range from 1.0×10^{-6} to 0.1 mol kg^{-1} with a low detection limit of 2.8×10^{-7} mol kg^{-1}, high selectivity, and little pH influence. The as-prepared electrode was used for the detection of the $[C_6mim]^+$ in distilled water, tap water, and river water with a good recovery. It was also successfully applied in the determination of mean activity coefficients of $[C_6mim]Br$ in fructose + water systems based on the potentiometric method at 298.15 K.

Keywords Ionic liquid · Molecularly imprinted polymer · PVC membrane · Ion-selective electrode

Introduction

Ionic liquids (ILs) are a salt melting at about room temperature, which consist of organic cation and inorganic or organic anion. With the development of science and technology, further study of ILs has been made by scientists and engineers, especially ionic liquids based on the 1-alkyl-3-methylimidazolium cations ($[C_nmim]X$, n = 2, 3, 4,…; X = Cl^-, Br^-, $[PF_6]^-$, $[BF_4]^-$, etc.). At present, a variety of $[C_nmim]X$ has been synthesized [1–3]. Then, various properties, such as hydrophobicity, viscosity, and density for pure $[C_nmim]X$ and their multicomponent systems, have been studied as well as the dependence of these properties on the side alkyl chains of cations and structure of anions [4–8]. Due to their unique physicochemical properties [9–12], $[C_nmim]X$ ILs have shown wide application in chemical sensors, extractive separation, catalysis, organic and inorganic synthesis, nanomaterial synthesis, and enzymatic reactions and become a research hotspot.

However, recently, many researches have indicated that $[C_nmim]X$ have bad effects (such as acute and chronic toxicity reaction, induction of teratogenesis and mutagenesis) on plant [13], microbe [14], and test animal [15–17] in certain experiment conditions. Thus, they may have different degrees of potential toxicity to the human body and environment [18–20]. Their large-scale use would give rise to environmental pollution through accidental spills or effluents. The determination of $[C_nmim]X$ in aqueous solution is a basis to

Electronic supplementary material The online version of this article (doi:10.1007/s11581-016-1708-z) contains supplementary material, which is available to authorized users.

✉ Kelei Zhuo
klzhuo@263.net; kzhuo@htu.cn

[1] Collaborative Innovation Center of Henan Province for Green Manufacturing of Fine Chemicals, Key Laboratory of Green Chemical Media and Reactions, Ministry of Education, School of Chemistry and Chemical Engineering, Henan Normal University, Xinxiang, Henan 453007, People's Republic of China

accurately assess their environmental impact, physicochemical properties. Therefore, it is essential to develop an efficient method for the determination of [$C_n$mim]X.

Up to now, the conventional methods for determining [$C_n$mim]X are chromatography and electrophoresis [21, 22], which have excellent sensitivity. But these methods have some drawbacks such as complex sample pretreatment, time consuming, lack of in situ measurement ability, and high testing costs or expensive apparatuses. PVC membrane electrodes [23] and carbon paste electrodes [24] have also been used for the determination of [$C_n$mim]X [25–27]. But the selectivity of the sensors is not very good. Therefore, it is desirable to develop a simple, reliable, well-selective, and environment-friendly method for the detection of [$C_n$mim]X in environmental and biological samples. Because potentiometric sensors are easy-to-use devices that allow rapidly and accurately qualitative or quantitative analysis at relatively low concentration, thus, the potentiometric sensor has attracted much interest over these years and then the advance in the field of molecular imprinting technology (MIT) makes it more promising in the modern laboratory.

MIT, a novel molecular recognition technology, can be used for the preparation of MIPs. MIPs completely match with the template on three-dimensional structure and thus are prior to extract the template compared to other interfering ions. As the recognition element or modification reagent, MIPs are a promising material in the field of potentiometric sensors [28–31]. These sensitive membrane systems of potentiometric sensors mainly include traditional systems, self-assembled systems, embedded systems, electrical aggregation systems, and sol-gel systems [32, 33]. The commonly used membrane system is an embedded system by dispersing MIPs in PVC matrix or carbon paste [30]. The as-prepared sensor is simple and easy to follow and has wide application.

In this work, a potentiometric sensor was fabricated by dispersing MIPs into plasticized PVC matrix and used for the determination of $[C_6mim]^+$ in aqueous solution. The as-prepared electrode exhibited a Nernstian response (58.87 mV per decade) to $[C_6mim]^+$ in a concentration range from 1.0×10^{-6} to 0.1 mol kg^{-1} with a low detection limit of 2.8×10^{-7} mol kg^{-1}, high selectivity, and little pH influence. The as-prepared electrode was successfully applied in the detection of the $[C_6mim]^+$ in distilled water, tap water, and river water. Moreover, the electrode can also be used successfully in the determination of mean activity coefficients of [C_6mim]Br in fructose + water systems by using the potentiometric method.

Experimental

Apparatus and reagents

Fourier transform infrared (FTIR) spectra were recorded on a Nicolet 6700 spectrophotometer, and scanning electron microscopy (SEM) measurements were obtained on a JSM-6390LV scanning electron microscope (Japan Electron Company). Thermogravimetric analyses (TGA) were done using a Netzsch Sta 449 C thermal analyzer.

Ionic liquids [C_6mim]Cl, [$C_n$mim]Br (n = 2–8, 10, 12, 14, and 16; >99 %), [C_nPy]Br (n = 2, 4; >99 %), and tetrabutylphosphonium bromide ([P_{4444}]Br, 99 %) were purchased from Lanzhou Greenchem. Co., LICP, China. Dibutyl phthalate (DBP, >98.5 %), choline chloride (ChCl, >98 %), tetramethylammonium bromide (TMAB, ≥98 %), tetraethylammonium bromide (TEAB, ≥98 %), hexadecyltrimethyl ammonium bromide (CTAB, ≥99 %), bis(2-ethylhexyl) sebacate (DOS, ≥97 %), acetophenone (≥98 %), and polyvinyl-chloride (PVC) were purchased from Aladdin. Tetrahydrofuran (THF) and inorganic salts were purchased from Tianjin Chem. Co., China. THF was redistilled in the presence of sodium before use. Methacrylic acid (MAA, ≥99 %), ethylene glycol dimethacrylate (EGDMA, ≥99 %), and 2,2′-azobisisobutyronitrile (AIBN, ≥99 %) were from J&K Chemical Company, China. MAA was distilled in vacuum to remove stabilizers prior to use. All these materials were dried under vacuum for a few days before use. Butyl-(2-hydroxyethyl)-dimethylammonium bromide ([C_4DMEA]Br) and decyl-(2-hydroxyethyl)-dimethylammonium bromide ([C_{10}DMEA]Br) were synthesized according to the procedures described in the literature [34]. Double-distilled water with conductivity of 1.0–1.5 μs cm^{-1} was used throughout all experiments.

Synthesis of the imprinted and non-imprinted polymers

Synthesis route of molecularly imprinted polymer (MIP) particles for $[C_6mim]^+$ is shown in Fig. 1. MIP particles for $[C_6mim]^+$ were prepared by taking 0.50 mmol of [C_6mim]Cl, 2.00 mmol of functional monomer (MAA), and 50 mL acetonitrile into a 250-mL flask. Subsequently, 7.00 mmol of cross-linker (EGDMA) was added. The mixture was left in contact for 6 h for prearrangement and followed by adding 0.06 mmol of initiator (AIBN). Then, the mixture was sonicated for 10 min to maintain homogeneity and was purged with Ar for 15 min for anaerobic process. The flask was sealed under this atmosphere. It was then kept stirring in a water bath maintained at 60 °C to start the polymerization process. After 24 h, the template and unpolymerized monomers were removed by Soxhlet extraction with 150 mL of methanol/acetic acid (4/1, v/v) by refluxing for 48 h.

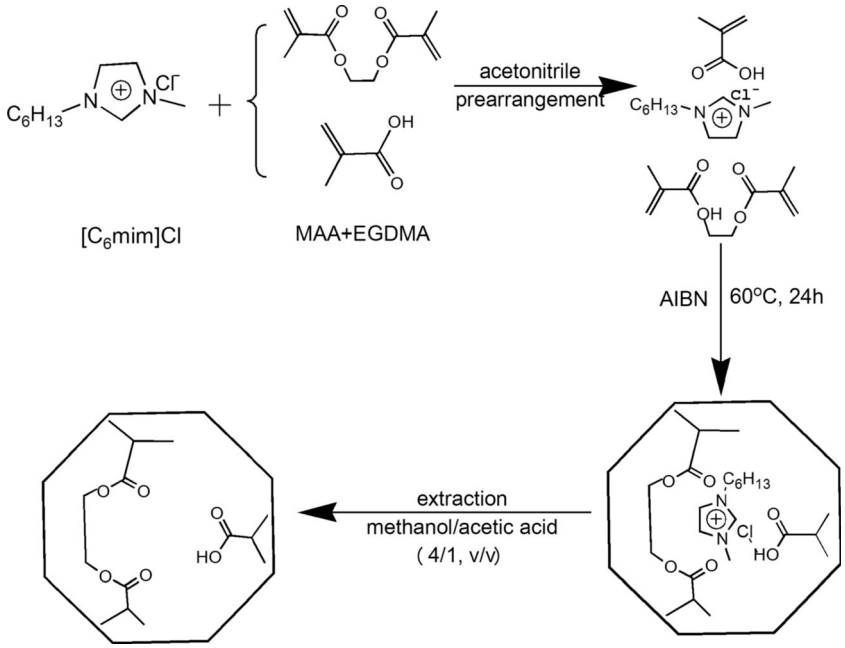

Fig. 1 Synthesis route of molecularly imprinted polymer particles for $[C_6mim]^+$

Then, the particles were methanol-washed until neutral. The resulting MIP particles were dried to a constant weight under vacuum at 60 °C and were used in the following experiments. Non-imprinted polymer (NIP) particles were prepared analogously without the addition of template during the polymer material preparation.

Preparation of the MIP-based potentiometric sensor

The molecularly imprinted polymer-based potentiometric sensor was prepared as follows: powdered PVC (100 mg), MIP (4 mg), and DBP (189 mg) were dissolved in dry freshly distilled THF (5 mL). After ultrasonic mixing for 3 min, the resulting solution was poured into a glass ring (ca. 1.8 cm in diam.) until a homogeneous transparent membrane (ca. 0.4 mm in thickness) was obtained by evaporation at room temperature. The membrane was cut into small rounds (ca. 1.1 cm in diam.) using a hole punch, and subsequently, the small rounds were glued into the end of the custom-machined electrode bodies with THF. Eight hundred microliters inner filling solution (containing 1.0×10^{-2} mol kg^{-1} $[C_6mim]Cl$ and 1.0×10^{-2} mol kg^{-1} NaCl) was added into the electrode body with an AgCl-coated Ag wire as the internal reference electrode. An electrochemical cell was fabricated by immersing the as-prepared electrode and an external reference electrode (AgCl-coated Ag wire) into a sample solution. The preparation of the MIP-based potentiometric sensor is shown in Fig. 2. Prior to potentiometric measurements, the as-prepared electrodes were conditioned for 24 h in $[C_6mim]Br$ solution (1.0×10^{-2} mol kg^{-1}). When not in use, the electrodes were kept in the same solution.

Results and discussion

Characterization of MIP particles

FTIR characterization

FTIR spectra are presented in Fig. 3. It can be clearly seen that the FTIR spectra of MIP and NIP were similar. In the FTIR spectrum of $[C_6mim]Cl$, the absorptions were observed as follows: C–H stretching in imidazolium ring (~3044 cm^{-1}), C–H stretching of alkyl chain in imidazolium ring (~2954, ~2929, ~2858 cm^{-1}), C=C stretching (~1569 cm^{-1}), C=N stretching (~1460 cm^{-1}), in-plane vibration of imidazolium ring (~1169 cm^{-1}), and aromatic C–H out of plane bending bands (~837, ~765 cm^{-1}). The peaks at ~2983 cm^{-1}, ~2952 m^{-1}, and ~1637 cm^{-1}, which are characteristic of $[C_6mim]Cl$, were observed in the unleached MIP, indicating that $[C_6mim]Cl$ existed in the unleached MIP. However, the intensities of these spectra were significantly diminished probably because of the interaction between $[C_6mim]Cl$ and MAA/EGDMA. Meanwhile, these spectra were not seen in the leached MIP. In addition, the spectra in leached MIP and NIP were similar. This proved that the target molecule ($[C_6mim]Cl$) had been efficiently leached from MIP in the solvent elution step.

TGA characterization

TGA plots of the leached MIP, unleached MIP, and NIP particles are depicted in Fig. 4. The thermal stability and the weight loss of the prepared polymers were measured up to 800 °C. The three polymers had similar patterns related to

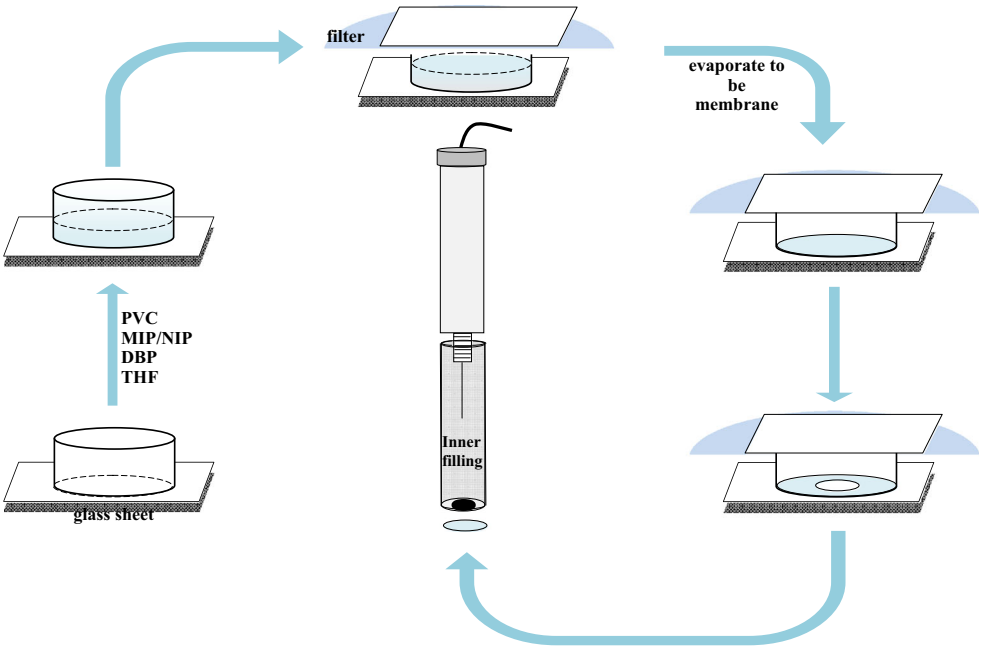

Fig. 2 The fabrication of the MIP-based potentiometric sensor

the decomposition of monomer and the cross-linker, and were completely decomposed by reaching 500 °C. However, for the unleached MIP particles, there was a mass loss between 250 and 300 °C, assigned to the decomposition of [C_6mim]Cl since the decomposition temperature is 253 °C.

SEM characterization

Figure 5 shows the morphologies of leached MIP (a), unleached MIP (b), and NIP particles (c). Different morphologies were observed for MIP and NIP particles. NIP particles displayed very uniform polymer microspheres with an average diameter of 0.65 μm. However, both leached MIP and unleached MIP particles had not obvious spherical contour instead of slices and cloud-like. This phenomenon indicates that the template molecule plays an important role in the growth of the particles in the precipitation polymerization. This can be explained as follows: the MAA (functional monomer) may exist in different forms in the MIP and NIP reaction systems. In the reaction system for NIP without the template molecular, MAA can form dimers through intermolecular hydrogen bonds. Both single MAA and MAA dimers can take part in the pre-polymerization. In the reaction system for MIP, however, there is an additional molecular interaction between MAA and the template molecule ([C_6mim]Cl), which might somehow influence the growth of the cross-linked polymer [35].

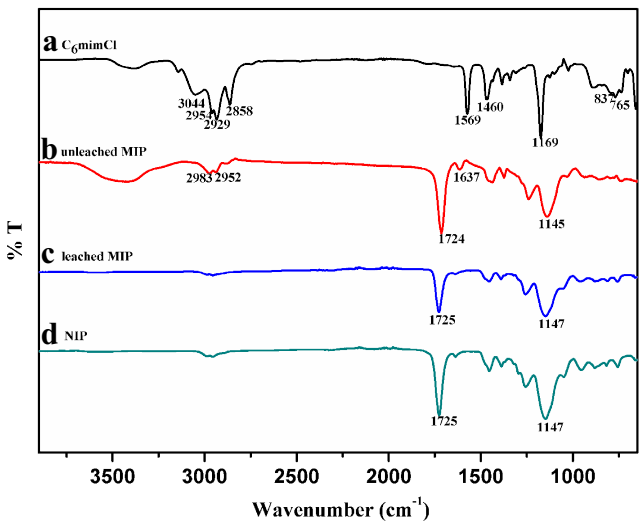

Fig. 3 FTIR spectra of [C_6mim]Cl (**a**), unleached MIP (**b**), leached MIP (**c**), and NIP (**d**) particles

MIP-based sensor composition selection

For potentiometric sensors, the recognition element embedded in the sensing component of the electrode is a key factor to

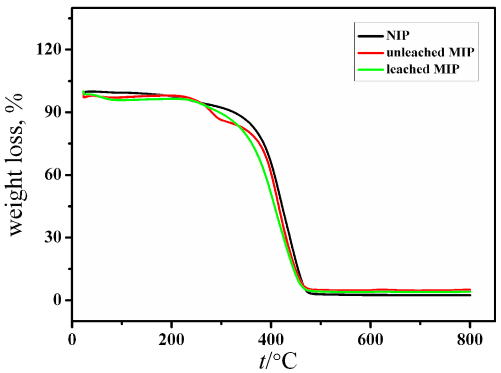

Fig. 4 TG plots of the leached MIP (*green line*), unleached MIP (*red line*), and NIP (*black line*) particles

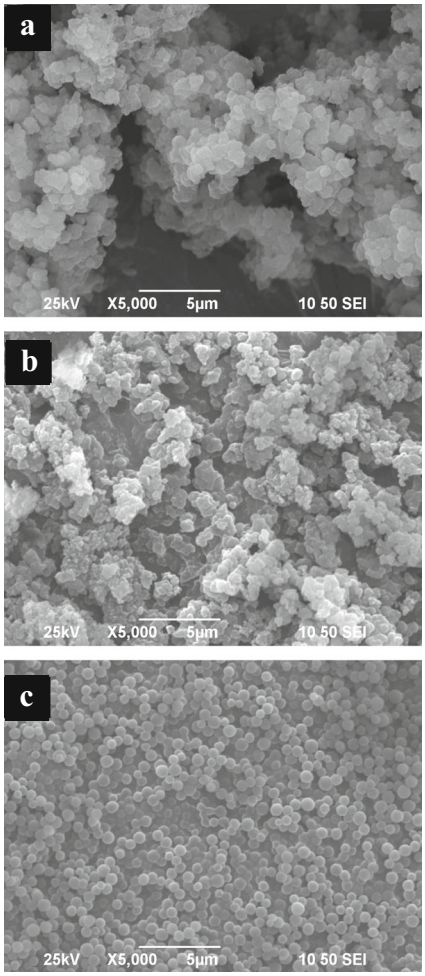

Fig. 5 SEM images of leached MIP (**a**), unleached MIP (**b**), and NIP (**c**)

determine the sensitivity and selectivity. However, the influences of the membrane composition, the nature of solvents, and the type of additives cannot be ignored. Here, the MIP as the recognition element was used to fabricate different sensors (the potentiometric sensor for $[C_6mim]^+$) with a variety of membrane compositions (PVC, plasticizer, and additives). The influences of the factors were studied and the results for these sensors are given in Table 1.

It is usually believed that as a component of sensor membranes, a lipophilic cationic additive not only provides cation binding sites to enhance the sensitivity but also reduces the electrode membrane impedance. However, herein, the electrodes without additives showed superior performance compared to the electrodes with additives such as tetraphenylboron sodium (NaTPB), sodium fluoroborate ($NaBF_4$), and potassium hexafluorophosphate (KPF_6). Obviously, the electrodes without additives (Nos. 5–19) had lower detection limit than the electrodes with NaTPB additives (Nos. 1–4). Next, we give the following explanations. Firstly, if NaTPB has an interaction with MIP particles, the existence of NaTPB would prevent the interaction between the MIP particles and the target molecules. So, the response of the electrode with NaTPB additive to the target molecule decreases, resulting in a higher detection limit. Secondly, if NaTPB has no interaction with MIP particles, the existence of NaTPB would decrease the recognition sites on the membrane surface. Although NaTPB may also have a response to the target molecule, the response is not stronger than that of MIP. Therefore, the detection limit of the electrode with NaTPB additives is higher. For the electrodes with additives ($NaBF_4$ and KPF_6), there was no good linear relationship between E and lg$c$ (E, cell potention; c, the concentration of target molecule), and thus, the data have not been presented in Table 1.

The response of the electrodes (Nos. 5–9) showed no significant change with the increase of MIP, indicating that the electrode (No. 7) had the best performance. When the amount of MIP was fixed at 4 mg, the response of the electrodes (Nos. 7, 10–14) was studied by changing the amount of the plasticizer (DBP). The electrode (No. 7) showed the best performance. Meanwhile, the response of the electrodes (Nos. 15–17) was also studied by changing the amount of PVC, indicating that the electrode (No. 16) had the best performance.

The addition of plasticizers can enhance the sensitivity of polymeric membrane sensors, and the effect of plasticizers on electrode film properties is most likely dependent on the material-plasticizer compatibility. But now, there has not been a standard method to evaluate the compatibility. The dielectric constant of plasticizers can be used as a criterion. According to the research on polyvinyl-chloride (PVC), the plasticizers with dielectric constant (ε = 4–8) is better. In addition, the plasticizers with a low permittivity may cause the lower conductivity of as-prepared electrode film [36]. So, in this work, we chose DBP (ε = 8.5) as plasticizer. As emphasized, the dielectric constant of plasticizers is not the only criterion. We should consider all factors, such as the compatibility, conductivity, lipophilicity, high molecular weight, viscosity, and response performance. The electrode (No. 16) with DBP (moderate dielectric constant, ε = 8.5) showed better performance than electrodes with DOS (lower dielectric constant, ε = 4) or acetophenone (higher dielectric constant, ε = 17.4). The performance of the electrodes containing acetophenone was the worst because the membrane was non-transparent and poorly flexible, which largely affects the response to the target molecule.

The electrodes with NIP did not show better performance than those with MIP (sub-Nernstian slope 48–52 mV per decade). This is mainly because the response of the electrodes with MIP comes from two sources [28]. One is the interaction between the target molecule and the selective sites (the imprinted cavities on the surface of the MIP). This part of the interaction is named as the site interaction. The other is the interaction of the target molecule with the bulk of the MIP and sensor membrane besides the site interaction. This part of

Table 1 Optimization composition of the MIP based potentiometric sensors for $C_6mim]^+$

No.	Composition (mg)						Slope (mV/dec)	Line range (mol kg^{-1})
	PVC	MIP	DBP	NaTPB	DOS	Acetophenone		
1	95	4	185	4	–	–	52.5 ± 0.1	1.0×10^{-5}–0.1
2	95	5	185	3	–	–	53.5 ± 0.1	1.0×10^{-5}–0.1
3	95	6	185	2	–	–	52.5 ± 0.3	1.0×10^{-5}–0.1
4	95	7	185	1	–	–	55.7 ± 0.2	1.0×10^{-5}–0.1
5	95	2	191	–	–	–	54.7 ± 0.3	1.0×10^{-6}–0.1
6	95	3	190	–	–	–	53.3 ± 0.1	1.0×10^{-6}–0.1
7	95	4	189	–	–	–	54.9 ± 0.1	1.0×10^{-6}–0.1
8	95	6	187	–	–	–	51.3 ± 0.2	1.0×10^{-6}–0.1
9	95	8	185	–	–	–	53.0 ± 0.3	1.0×10^{-6}–0.1
10	95	4	186	–	–	–	53.4 ± 0.3	1.0×10^{-6}–0.1
11	95	4	191	–	–	–	54.0 ± 0.2	1.0×10^{-6}–0.1
12	95	4	193	–	–	–	54.0 ± 0.2	1.0×10^{-6}–0.1
13	95	4	195	–	–	–	54.1 ± 0.1	1.0×10^{-6}–0.1
14	95	4	196	–	–	–	54.3 ± 0.3	1.0×10^{-6}–0.1
15	85	4	189	–	–	–	52.4 ± 0.3	1.0×10^{-6}–0.1
16	100	4	189	–	–	–	58.9 ± 0.3	1.0×10^{-6}–0.1
17	105	4	189	–	–	–	56.2 ± 0.2	1.0×10^{-6}–0.1
18	100	4	–	–	189	–	56.3 ± 0.2	1.0×10^{-6}–0.1
19	100	4	–	–	–	189	–	–

the interaction is named as the surface adsorption. But, for the electrodes with NIP, the response is only through the second effect because the electrodes with NIP have no predesigned binding sites.

Finally, the electrode (No. 16) was chosen for further examination. The best composition of the electrode is fixed to be 100 mg of PVC, 4 mg of MIP, and 189 mg of DBP.

Characteristics of the MIP-modified electrode

Calibration graph and statistical data

The MIP-modified electrode with the optimum composition (No. 16) exhibited a Nernstian response to $[C_6mim]^+$ in aqueous solution in the range from 1.0×10^{-6} to 0.1 mol kg^{-1}, and the slope was 58.87 mV per decade (Fig. 6). The detection limit of the electrode was evaluated to be 2.8×10^{-7} mol kg^{-1} by extrapolation of the linear portion of the electrode's calibration curve.

Selectivity of the MIP-modified electrode

Selectivity, one of the most important features for ion-selective electrode, describes the electrode's monitoring accuracy to the target ion in the presence of interfering ions. In this work, the selectivity coefficient of the novel MIP-modified electrode was determined by the separate solution method (SSM) [37, 38]. The selectivity coefficients were calculated by the following equation:

$$\log K_{ij}^{pot} = \frac{E_2 - E_1}{2.303RT/Z_iF} + \left(1 - \frac{Z_i}{Z_j}\right)\log a_i$$

where E_1, E_2, Z_i, and Z_j are the measured potentials and charges on the ions i and j. a_i is the activity of target ion i (but no j) and j is the interfering ion at the same activity $a_j = a_i$ (but no i). The resulting values of selectivity coefficients are listed in Table 2. For the alkylmethylimidazolium cations, the extent of interference is strengthened, when the number of carbon atoms of alkyl side chain of the interfering ions increases ($[C_nmim]^+$, n = 2–8, 10, and 12). With the increase of the length of alkyl side chain, the hydrophobicity of

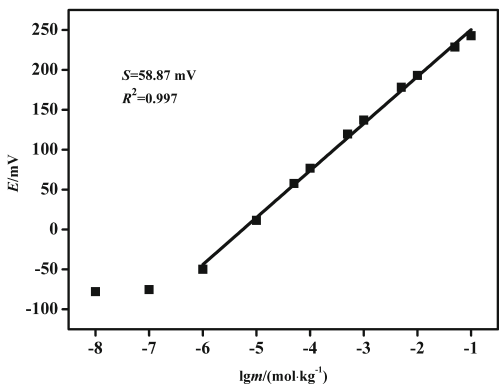

Fig. 6 Calibration curve of the MIP-modified electrode for $[C_6mim]^+$ (No. 16)

Table 2 Logarithm of selective coefficients (KSSM) of the electrode (No. 16) to 1-hexyl-3-methylimidazolium cation ($[C_6mim]^+$) for various interfering cations

Interfering cation	lgK_{SSM}	Interfering cation	lgK_{SSM}
$[C_2mim]^+$	−1.99	Na^+	−2.38
$[C_3mim]^+$	−1.50	K^+	−3.19
$[C_4mim]^+$	−0.98	NH_4^+	−3.38
$[C_5mim]^+$	−0.39	Ca^{2+}	−5.00
$[C_6mim]^+$	0	Mg^{2+}	−4.82
$[C_7mim]^+$	0.82	Zn^{2+}	−5.02
$[C_8mim]^+$	1.13	Cu^{2+}	−4.85
$[C_{10}mim]^+$	2.43	ChCl	−2.47
$[C_{12}mim]^+$	3.41	$[C_4DMEA]^+$	−1.56
$[C_{14}mim]^+$	3.77	$[C_{10}DMEA]^+$	2.48
$[C_{16}mim]^+$	3.97	TMAB	−1.74
C_2PyBr	0.67	TEAB	−1.34
C_4PyBr	−0.29	CTAB	3.61
		$[p_{4444}]^+$	2.71

interfering ions increases, and the interfering ions trend to be transferred into the membrane phase from aqueous solution because. In addition, the logarithmic selectivity coefficients of the electrode increase linearly (Fig. S3). Obviously, the special regular is in accord with the Hofmeister series [39]. Pyridinium cations have similar structures with alkylmethylimidazolium cations (both cations contain cyclic conjugated systems). Pyridinium cations interfere the response of the electrode to $[C_6mim]^+$ at a certain extent. The interference of $[C_2Py]^+$ is higher than that of $[C_4Py]^+$ because $[C_2Py]^+$ is easier to enter the designed cavity. $[C_nDMEA]^+$ is more hydrophilic than other types of ionic liquid cations with the same number of carbon atoms due to the hydroxyl groups on its branched chain. So, the interference of $[C_4DMEA]^+$ is relatively smaller than that of $[C_4mim]^+$. For quaternary ammonium cations, the interference of TMAB and TEAB is relatively smaller than that of CTAB. $[p_{4444}]^+$ is highly symmetrical in structure and thus has a bigger interference. For the inorganic cations, the interference of divalent cations (Ca^{2+}, Mg^{2+}, Zn^{2+}, and Cu^{2+}) are lower than that of univalent inorganic cations (Na^+, K^+, and NH_4^+). Obviously, inorganic cations hardly have interference to the target molecule $[C_6mim]^+$. Overall, the electrode shows a good selectivity especially for inorganic cations as the interference ions.

pH effect on the electrode response

The effect of pH on the response of the MIP-modified sensor was studied over the pH range from 2 to 12. The pH values of given concentration solutions ($[C_6mim]Br$) were adjusted by adding the prepared HCl or NaOH solution. The potential variation as a function of pH is plotted (Fig. 7). The results

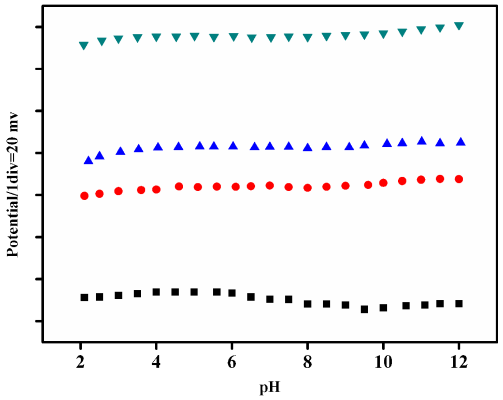

Fig. 7 Effects of pH on the potential response of the electrode (No. 16) for $[C_6mim]^+$ at m_{IL}/ = mol kg^{-1} (5×10^{-5} (*black square*), 5×10^{-4} (*red circle*), 1×10^{-3} (*blue up-pointing triangle*), and 1×10^{-2} (*green down-pointing triangle*))

indicated that pH has little influence on the potential response and the electrode can be used in a wide pH range. This is mainly because the structure of the target ion has not obvious change under acidic or alkaline condition ($[C_6mim]Br$ exists in the form of $[C_6mim]^+$ and Br^- in water samples. The target ion ($[C_6mim]^+$) does not form precipitates or chelate complexes with other ions).

Response time and life-time of the MIP-modified electrode

The response time, another important factor for the ion-selective electrode, describes the average equilibrium time reached in early stage of contacting analyte. In this work, the response time for the electrode (No. 16) was recorded upon changing the concentration of $[C_6mim]Br$ solution from 1.0×10^{-8} to 0.1 mol kg^{-1} to achieve a value within ±1 mV. The response time of the electrode was approximately equal to 3 min. Moreover, the as-prepared MIP-modified electrode can be used for at least 3 months.

Repeatability and reproducibility

The repeatability of the MIP-modified electrode was studied by three measurements with the same electrode over the working concentration ranges. For the three replicate measurements, the standard deviation (SD) of Nernstian slope of the electrode obtained was 0.3 mV, showing a good repeatability of the potential response.

The reproducibility of the MIP-modified electrode was tested by five electrodes which were prepared by the same method and same optimized membrane composition. The measured Nernstian slopes of the five electrodes were respectively 59.14, 59.16, 57.55, 57.20, and 58.32 mV, with a SD of 0.9 mV.

Table 3 Determination of $[C_6mim]Br$ by the prepared electrode (No. 16) in the real samples

Samples	Content of $[C_6mim]Br$ (mol kg^{-1})	%Recovery ± SD[a]
Distilled water	2.045×10^{-5}	99.6 ± 0.4
	4.025×10^{-5}	100.8 ± 0.1
	6.087×10^{-5}	99.4 ± 0.5
	7.962×10^{-5}	101.5 ± 0.1
	2.007×10^{-4}	102.5 ± 0.3
	4.002×10^{-4}	104.1 ± 0.2
	5.967×10^{-4}	104.4 ± 0.3
	8.007×10^{-4}	104.9 ± 0.3
Tap water	2.020×10^{-5}	98.9 ± 0.5
	4.061×10^{-5}	98.7 ± 0.4
	5.989×10^{-5}	99.8 ± 0.4
	8.126×10^{-5}	99.9 ± 0.4
	1.943×10^{-4}	101.3 ± 0.7
	3.989×10^{-4}	102.3 ± 0.5
	5.969×10^{-4}	102.7 ± 0.4
	8.023×10^{-4}	103.4 ± 0.4
River water	2.018×10^{-5}	101.8 ± 0.8
	3.821×10^{-5}	101.6 ± 0.6
	5.979×10^{-5}	101.1 ± 0.4
	8.798×10^{-5}	101.6 ± 0.7
	1.989×10^{-5}	102.7 ± 0.5
	4.033×10^{-4}	104.5 ± 0.7
	5.941×10^{-4}	103.6 ± 0.4
	7.999×10^{-4}	105.0 ± 0.5

[a] Mean of three determinations, SD is the standard deviation

Analytical application

The MIP-modified electrode was successfully applied for the determination of $[C_6mim]Br$ in distilled water, tap water, and river water, respectively. The analysis was recorded by the standard addition method. The recoveries are in the range of 98.73–104.98 % (Table 3). Therefore, the potentiometric sensor can provide a good alternative for the determination of $[C_6mim]^+$ in real samples.

On the basis of the previous work, the MIP-modified electrode was also used to study the mean activity coefficients for $[C_6mim]Br$ in water and fructose + water mixtures at T = 298.15 K. The results are shown in Table S1, which is fairly accorded with those reported in the literature [40].

The MIP-modified electrode can not only be used in the determination of $[C_6mim]Br$ in real samples but also be popularized and applied for the determination of their thermodynamic properties in various water samples.

Conclusions

The MIP-modified electrode, MIP as the recognition element, was fabricated for the determination of $[C_6mim]^+$. The as-prepared electrode exhibited a good selectivity for inorganic cations as the interference ions. The pH had little influence on the response of the electrode. The novel electrode was successfully applied for the determination of $[C_6mim]Br$ in real water samples with good recoveries. In addition, the MIP-modified electrode was also used to determine the mean activity coefficients for $[C_6mim]Br$ in water and fructose + water mixtures, which are in good consistence with the literature. We believe that the electrode would be applied widely to the detection of ILs in other systems and the determination of thermodynamic properties of ILs in solutions.

Acknowledgments Financial supports from the National Natural Science Foundation of China (Nos. 21173070, 21303044, and 21573058), Program for Innovative Research Team in Science and Technology in University of Henan Province (15IRTSTHN 003), and Key scientific research project of Henan province higher education of China (No. 15A150058) are gratefully acknowledged.

References

1. Wilkes JS, Levisky JA, Wilson RA, Hussey CL (1982) Dialkylimidazolium chloroaluminate melts: a new class of room-temperature ionic liquids for electrochemistry, spectroscopy and synthesis. Inorg Chem 21(3):1263–1264
2. Hussey CL (1988) Room temperature haloaluminate ionic liquids. Novel solvents for transition metal solution chemistry. Pure Appl Chem 60(12):1763–1772
3. Wilkes JS, Zaworotko MJ (1992) Air and water stable 1-ethyl-3-methylimidazolium based ionic liquids. J Chem Soc Chem Commun 13:965–966
4. Bai L, Li SN, Zhai QG, Jiang YC, Hu MC (2015) Density, refractive index, and viscosity of binary systems composed of ionic liquids (C(n)mim Cl, n = 2, 4) and three dipolar aprotic solvents at T = 288.15-318.15 K. Chem Pap 69(10):1378–1388
5. Sastry NV, Vaghela NM, Macwan PM (2013) Densities, excess molar and partial molar volumes for water + 1-butyl- or, 1-hexyl- or, 1-octyl-3-methylimidazolium halide room temperature ionic liquids at T = (298.15 and 308.15) K. J Mol Liq 180:12–18
6. Sadeghi R, Ebrahimi N (2011) Ionic association and solvation of the ionic liquid 1-hexyl-3-methylimidazolium chloride in molecular solvents revealed by vapor pressure osmometry, conductometry, volumetry, and acoustic measurements. J Phys Chem B 115(45): 13227–13240
7. Lu S, Brennecke JF (2015) Characterization of imidazolium chloride ionic liquids plus trivalent chromium chloride for chromium electroplating. Ind Eng Chem Res 54(17):4879–4890
8. Zhang L, Zhang Q, Li JH (2007) Electrochemical behaviors and spectral studies of ionic liquid (1-butyl-3-methylimidazolium tetrafluoroborate) based sol–gel electrode. J Electroanal Chem 603(2): 243–248
9. Plechkova NV, Seddon KR (2008) Applications of ionic liquids in the chemical industry. Chem Soc Rev 37(1):123–150
10. Zhao YS, Bostrom T (2015) Application of ionic liquids in solar cells and batteries: a review. Curr Org Chem 19(6):556–566

11. Petkovic M, Seddon KR, Rebelo LP, Silva Pereira C (2011) Ionic liquids: a pathway to environmental acceptability. Chem Soc Rev 40(3):1383–1403
12. Liu HT, Liu Y, Li JH (2010) Ionic liquids in surface electrochemistry. Phys Chem Chem Phys 12(8):1685–1697
13. Latala A, Stepnowski P, Nedzi M, Mrozik W (2005) Marine toxicity assessment of imidazolium ionic liquids: acute effects on the Baltic algae Oocystis submarina and Cyclotella meneghiniana. Aquat Toxicol 73(1):91–98
14. Docherty KM, Kulpa CF (2005) Toxicity and antimicrobial activity of imidazolium and pyridinium ionic liquids. Green Chem 7(4): 185–189
15. Pretti C, Chiappe C, Pieraccini D, Gregori M, Abramo F, Monni G, Intorre L (2006) Acute toxicity of ionic liquids to the zebrafish (Danio rerio). Green Chem 8(3):238–240
16. Bernot RJ, Kennedy EE, Lamberti GA (2005) Effects of ionic liquids on the survival, movement, and feeding behavior of the freshwater snail, Physa acuta. Environ Toxicol Chem 24(7):1759–1765
17. Bernot RJ, Brueseke MA, Evans-White MA, Lamberti GA (2005) Acute and chronic toxicity of imidazolium-based ionic liquids on Daphnia magna. Environ Toxicol Chem 24(1):87–92
18. Ke M, Zhou AG, Song ZZ, Jiang QZ (2007) Toxicity of ionic liquids. Progress in Chemistry 19(5):671–679
19. Stepnowski P, Skladanowski AC, Ludwiczak A, Laczynska E (2004) Evaluating the cytotoxicity of ionic liquids using human cell line HeLa. Hum Exp Toxicol 23(11):513–517
20. Docherty KM, Hebbeler SZ, Kulpa CF Jr (2006) An assessment of ionic liquid mutagenicity using the Ames Test. Green Chem 8(6): 560–567
21. Stepnowski P (2006) Application of chromatographic and electrophoretic methods for the analysis of imidazolium and pyridinium cations as used in ionic liquids. Int J Mol Sci 7(11):497–509
22. Nichthauser J, Mrozik W, Markowska A, Stepnowski P (2009) Analysis of residual ionic liquids in environmental samples: development of extraction methods. Chemosphere 74(4):515–521
23. Wang JG, Wang LL, Han YH, Jia JB, Jiang LL, Yang WW, Sun QH, Lv H (2007) PVC membrane electrode based on triheptyl dodecyl ammonium iodide for the selective determination of molybdate(VI). Anal Chim Acta 589(1):33–38
24. Zhu YQ, Liu XJ, Jia JB (2015) Electrochemical detection of natural estrogens using a graphene/ordered mesoporous carbon modified carbon paste electrode. Anal Methods 7(20):8626–8631
25. Ortuno JA, Cuartero M, Garcia MS, Albero MI (2010) Response of an ion-selective electrode to butylmethylimidazolium and other ionic liquid cations. Applications in toxicological and bioremediation studies. Electrochim Acta 55(20):5598–5603
26. Zhuo KL, Wei YJ, Ma JJ, Chen YJ, Bai GY (2013) Response of PVC membrane ion-selective electrodes to alkylmethylimidazolium ionic liquid cations. Sensors and Actuators B-Chemical 186:461–465
27. Ma XL, Wang CF, Ren H, Chen YJ, Zhuo KL (2015) Response of a new multi-walled carbon nanotubes modified carbon paste electrode to 1-hexyl-3-methylimidazolium cation in aqueous solution. Ionics 21(9):2503–2510
28. Alizadeh T, Akhoundian M (2010) A novel potentiometric sensor for promethazine based on a molecularly imprinted polymer (MIP): the role of MIP structure on the sensor performance. Electrochim Acta 55(10):3477–3485
29. Liang RN, Song DA, Zhang RM, Qin W (2010) Potentiometric Sensing of Neutral Species Based on a Uniform-Sized Molecularly Imprinted Polymer as a Receptor. Angew Chem Int Ed 49(14):2556–2559
30. Algieri C, Drioli E, Guzzo L, Donato L (2014) Bio-mimetic sensors based on molecularly imprinted membranes. Sensors 14(8):13863–13912
31. Anirudhan TS, Alexander S (2014) Multiwalled carbon nanotube based molecular imprinted polymer for trace determination of 2,4-dichlorophenoxyaceticacid in natural water samples using a potentiometric method. Appl Surf Sci 303:180–186
32. Gao X, Fan J, Wang XL, Zhang YS (2013) Synthesis of a novel 1-ethyl-3-methylimidazolium chloride ionic liquid molecularly imprinted polymer and its properties of specific adsorption and solid phase extraction. Acta Chim Sin 71(10):1411–1420
33. Qiu CX, Xing YH, Yang WM, Zhou ZP, Wang YC, Liu H, Xu WZ (2015) Surface molecular imprinting on hybrid SiO2-coated CdTe nanocrystals for selective optosensing of bisphenol A and its optimal design. Appl Surf Sci 345:405–417
34. Domańska U, Bogel-Łukasik R (2005) Physicochemical properties and solubility of Alkyl-(2-hydroxyethyl)-dimethylammonium bromide. J Phys Chem B 109(24):12124–12132
35. Yoshimatsu K, Reimhult K, Krozer A, Mosbach K, Sode K, Ye L (2007) Uniform molecularly imprinted microspheres and nanoparticles prepared by precipitation polymerization: the control of particle size suitable for different analytical applications. Anal Chim Acta 584(1):112–121
36. Fang SU, Ping DW, Xiao SU (2001) Enhancement of both ionic conductivity and permittivity of the high polymer film P(EO)_n-CuBr_2 under hydrostatic pressure(Ii)-application of method to add plasticizer. Chinese Journal of High Pressure Physics.15:161–168
37. Buck RP, Lindner E (1994) IUPAC recommendations for nomenclature of ion-selective electrodes. Pure Appl Chem 66(12):2527–2536
38. Mikhelson KN (2013) Ion-selective electrodes, 2013 edn. Springer
39. Schaller U, Bakker E, Spichiger UE, Pretsch E (1994) Ionic additives for ion-selective electrodes based on electrically charged carriers. Anal Chem 66(3):391–398
40. Zhuo KL, Ren H, Wei YJ, Chen YJ, Ma JJ (2014) Activity coeffi-cients of C(n)mim Br (n = 3 to 8) ionic liquids in aqueous fructose solution at T = 298.15 K. J Chem Eng Data 59(3):640–648